Carbohydrate Polymers 97 (2013) 558–564

Contents lists available at SciVerse ScienceDirect

Carbohydrate Polymers

journal homepage: www.elsevier.com/locate/carbpol

Classification and kinetic analysis of viscosity growth processes for NaOH-gelatinized rice starches

Hisashi Yamamoto*, Nozomi Sawai, Kanako Seo

Department of Food Science and Nutrition, Faculty of Human Life and Science, Doshisha Women's College of Liberal Arts, Kamigyo-Ku, Kyoto 602-0893, Japan

ARTICLE INFO

Article history:
Received 4 December 2012
Received in revised form 18 March 2013
Accepted 22 April 2013
Available online 10 May 2013

Keywords:
Viscosity
Starch
Gelatinization
NaOH
Kinetic analysis

ABSTRACT

Using capillary viscometry, viscosity growth processes were studied for non-glutinous rice starches gelatinized with different NaOH solution concentrations. The viscosity–time data series generally conformed to sigmoid curves with an arbitrary inflection point (IP) for each curve, and were analyzed using a kinetic model that incorporated a first-order reaction rate equation and a mixing rule of a power-law type. The shapes of curves were classified with the exponent ν or the ratio η^*/η_G, where η^* and η_G were viscosities at IP and at equilibrium, respectively. It was argued that these parameters were related to the complex formation arising from NaOH-starch interactions. The rate constant K defined uniformly for an entire process increased with NaOH concentration and was power-law dependent. Furthermore, it was suggested that gelatinization evolved non-uniformly over time. A non-uniform analysis was then performed by disassembling the entire process into several elementary stages and revealed the evolutionary process for K.

1. Introduction

Gelatinization is a reaction phenomenon commonly observed with starches and plays an important role not only in cooking but also in various industrial applications such as food processing, paper manufacturing, and pharmaceuticals. Understanding the underlying processes is thus indispensable to process design and control, and is essential for clarifying the underlying reaction mechanism. To date, with the aim of elucidating gelatinization processes and rates, various kinetic studies have been conducted using rheological, enzymatic hydrolysis, loss of birefringence, DSC, NMR, and X-ray diffraction/scattering approaches (Lund, 1984; Vermeylen et al., 2006, and references therein).

Most gelatinization phenomena investigated occurred in heated water. In these cases, hydrogen bonds between starch chains in the granules are destroyed by thermal fluctuations and the high mobility of monomolecular water, which results in disrupting structural integrity, granule swelling, and crystallite melting. From the dynamic responses to temperature jumps, Marchant and Blanshard (1978) and French (1984) speculated that a gelatinization process is "semi-cooperative". That is, the swelling of an amorphous region (gelatinized portion) contributes to disrupting crystallites (ungelatinized portion). It is significant that these molecular-level changes lead to macroscopic changes such as increased viscosity.

However, gelatinization can occur in starch dispersions, even at room temperature, in the presence of certain chemicals, such as electrolytes (Jane, 1993), DMSO (Shon, Lim, & Yoo, 2005), and urea (Hebeish, El-Thalouth, & El-Kashouti, 1981). These chemical phenomena are noteworthy because they do not require additional thermal energy. The driving force is only because of the action of the added chemicals. For kinetic studies with rheological methods, these non-heated phenomena are technically advantageous. However, compared with gelatinization in hot water, only few investigations of such "cold" phenomena have been conducted.

With this as a motivation, one of the present authors (H.Y.) and collaborators recently studied the viscosity (η) growth of non-glutinous rice starch that was gelatinized by 0.146 M NaOH solution at 20 °C, and discovered novel kinetic characteristics (Yamamoto, Makita, Oki, & Otani, 2006; Yamamoto, Isozumi, & Sugitani, 2005). The first cited study used batch-type rotational viscometry and found an exponential increase in viscosity during the early stage of gelatinization. The next study conducted continuous capillary viscometry for dilute dispersions and found that complete viscosity–time data series generated sigmoid curves. Each curve had an inflection point (IP) at that viscosity (η^*) that was approximately 1/2 of the equilibrium value (η_G). This type of kinetic behavior has not been previously reported in the literature and is in clear contrast to the kinetic behaviors in heated water, which generate convex curves (Kubota, Hosokawa, Suzuki, & Hosaka, 1979).

* Corresponding author. Tel.: +81 75 251 4215; fax: +81 75 251 4215.
E-mail addresses: hyamamot@dwc.doshisha.ac.jp, spitz852000@yahoo.co.jp (H. Yamamoto).

0144-8617/$ – see front matter © 2013 Elsevier Ltd. All rights reserved.
http://dx.doi.org/10.1016/j.carbpol.2013.04.100

The subsequent studies confirmed that similar viscosity increases occurred with non-glutinous corn and wheat starches (Yamamoto, Kawakami, Kitagawa, & Yamagata, 2012; Yamamoto, Moriyasu, et al., 2012). This established that the sigmoid behavior was not specific to a particular plant origin, but had a physicochemical origin. Based on the concept of starch complex formation, a physicochemical hypothesis has been proposed to explain the origin of this sigmoid behavior (Yamamoto et al., 2006; Yamamoto, Kawakami, et al., 2012).

To analyze novel viscosity–time data series, a kinetic model was proposed to incorporate a first-order reaction equation for the degree of gelatinization and a mixing rule of the fluidity (η^{-1}) type (Yamamoto et al., 2006). This mixing rule is different from the viscosity (η) type that is known for gelatinization in heated water (Kubota et al., 1979). The model describes a viscosity–time curve with an IP located at $\eta^* = \eta_G/2$ and exponential increase during the early stage, which approximates the data obtained for NaOH gelatinization under these special conditions.

However, experimentally, the position of IP is expected to vary depending on the samples used and environmental conditions. There is no reason for the ratio η^*/η_G to remain in the vicinity of 0.50; rather, it should generally assume an arbitrary value. In this case, the model specified above would not work as a good approximation. This motivated one of the present authors to extend the kinetic model by incorporating a mixing rule of a general power-law (η^ν) type, in which the exponent ν assumes an arbitrary number (Yamamoto, 2006). This one-parameter generalization is expected to provide a comprehensive classification and allow kinetic analysis of a wide variety of viscosity–time data series.

Thus, in the present study, we applied this new generalized kinetic model to the viscosity–time data series obtained for rice starches that were gelatinized with varying NaOH solution concentrations.

2. Materials and methods

2.1. Sample preparation and capillary viscometry

We used the same type of rice starch powder that was used in previous studies. According to information from the manufacturer (Shimada Chemical Co., Niigata, Japan), starch was made from government-controlled rice and had a moisture content of 13.5± 0.5 %, protein of ≤0.3% and ash of 0.1%. The Japan Food Research Laboratories (Osaka, Japan) evaluated the lipid content to be 0.5%, and determined the amylose ratio to be 14% using amylose/amylopectin assay kit (Biocon Ltd., Japan; Megazyme International Ireland Ltd., Ireland).

Capillary viscometry was employed for dilute samples to maintain their Newtonian flow properties and to obtain non-scattered viscosity–time data series. We prepared 1.0% (w/w) starch dispersions using procedures described previously (Yamamoto et al., 2005), with modifications only for the concentrations of added NaOH and temperatures. A principal series of samples were dispersions at 10 °C and gelatinized with NaOH concentrations ranging from 0.130 to 0.160 M. To study temperature dependence, we prepared another series of samples gelatinized with a 0.146 M NaOH solution at 9 °C and 15 °C. We also prepared two exceptional samples gelatinized with lower NaOH solution concentrations, 0.110 M at 40 °C and 0.093 M at 50 °C, to observe the behavior at higher temperatures.

Using previously described procedures (Yamamoto et al., 2005), flow measurements were made continuously until the equilibrium state, and viscosity was calculated from an efflux time for each flow. To obtain detailed information on each viscosity growth, we conducted the flow measurements iteratively at as short intervals as possible. For each gelatinization condition, these experiments were repeated at least thrice. The results are presented as mean ± S.D. in Table 1.

2.2. Kinetic model

A complete description of the present kinetic model is provided elsewhere (Yamamoto, 2006). We only present its outline here. Following a traditional treatment (Lund, 1984), we regard gelatinization as a kind of first-order reaction process during which a portion of the ungelatinized part (UG) is converted to a gelatinized part (G) with the sum of the amounts of [UG] and [G] unchanged. Then, the degree of gelatinization defined as the ratio $x \equiv [G]/([UG]+[G])$ evolves from 0 (initiation at $t=0$) to 1 (equilibrium, formally at $t=\infty$), according to the first-order reaction equation: $dx/dt = K(1-x)$ for which K is a reaction rate constant. Its solution, $x(t) = 1-\exp(-Kt)$, satisfies $d^2x/dt^2 < 0$; the degree of gelatinization increases in a convex manner.

During gelatinization, a sample is a mixture of UG and G in which viscosity (η) is hypothesized to increase with the degree of gelatinization according to a mixing rule of the power-law type:

$$\eta^\nu(x) = (1-x)\,\eta_{UG}^\nu + x\,\eta_G^\nu, \tag{1}$$

where η_{UG} and η_G are constant viscosities associated with UG and G respectively, and an exponent ν controls the mixed sate of UG and G (i.e., the degree of influence of G on the viscosity η of total sample). At $\nu = 0$, Eq. (1) should be replaced by a logarithmic type or a "random distribution": $\eta = \eta_{UG}^{1-x}\,\eta_G^x$ (Woodside & Messmer, 1961).

Eq. (1) with the special cases provides the viscosity ($\nu = 1$) and fluidity ($\nu = -1$) types of the mixing rule previously used to describe gelatinization in hot water ($\nu = 1$) and in NaOH solutions of specific concentrations ($\nu = -1$). Below, we consider a general case in which the exponent ν assumes an arbitrary value and show what shapes of viscosity growth curves, $\eta(t)$, are reproduced when combined with the first-order reaction rate equation.

Inserting the solution into Eq. (1) provides the time evolution for viscosity:

$$\eta^\nu(t) = \eta_G^\nu + \eta_{UGG}^\nu\, e^{-Kt}, \tag{2}$$

where a new symbol, $\eta_{UGG}^\nu \equiv \eta_{UG}^\nu - \eta_G^\nu$, is introduced. It was proved (Yamamoto, 2006) that under the two conditions $\nu < 1$ and $\eta_{UG} < (1-\nu)^{1/\nu}\,\eta_G$, the viscosity growth curve described by Eq. (2) exhibited a sigmoid shape and had an IP at

$$\eta^* = (1-\nu)^{1/\nu}\,\eta_G. \tag{3}$$

This equation provides a one-to-one correspondence between a mixing exponent $\nu(<1)$ and the ratio η^*/η_G (the viscosity at IP relative to that at equilibrium). The ratio η^*/η_G or an exponent ν plays a key role in classifying the global shapes of observed viscosity growth curves.

In the actual kinetic analysis, applying a non-linear least-squares method to the measured η–t data series up to the equilibrium or maximum viscosity point, we determined 4 parameters η_{UG}, η_G, ν and K appearing in Eq. (2). The ratio η^*/η_G was obtained from ν by using Eq. (3).

For a given data, the rate constant K can be schematically shown by linearizing Eq. (2):

$$\ln(\eta^\nu - \eta_G^\nu) = \ln \eta_{UGG}^\nu - Kt \qquad (\nu < 0), \tag{4}$$

$$\ln(\eta_G^\nu - \eta^\nu) = \ln \eta_{GUG}^\nu - Kt \qquad (\nu > 0), \tag{5}$$

with $\eta_{GUG}^\nu \equiv \eta_G^\nu - \eta_{UG}^\nu = -\eta_{UGG}^\nu$. If we have information on η_G and ν in advance, we can estimate K and η_{UG} by plotting the left-hand side of Eq. (4) or (5) against time and using linear regression analysis.

Table 1
Characteristic values (mean ± S.D.) for viscosity growth data series under different gelatinization conditions. The values in the three lines where the symbol (2005) was added in the T column were obtained by reanalyzing previous data (Yamamoto et al., 2005) using the current method. The values of η^*/η_G in the last column were computed from the formula (3) as $(1-\nu)^{1/\nu}$.

T[°C]	[NaOH]	η_{UG} [mPa·s]	η_G [mPa·s]	ν	K[$\times 10^{-2}$min^{-1}]	η^*/η_G
9	0.146	0.95 ± 0.04	14.17 ± 0.75	−0.935 ± 0.332	9.84 ± 2.43	0.491 ± 0.036
	0.130	0.94 ± 0.14	11.23 ± 1.03	0.669 ± 0.016	0.82 ± 0.10	0.192 ± 0.006
	0.135	0.97 ± 0.13	12.99 ± 1.44	−0.026 ± 0.298	2.29 ± 1.10	0.368 ± 0.056
	0.140	1.02 ± 0.05	12.28 ± 0.89	−1.316 ± 0.098	9.27 ± 1.39	0.528 ± 0.008
10	0.146	0.89 ± 0.02	13.72 ± 0.96	−0.923 ± 0.213	11.15 ± 2.16	0.491 ± 0.021
	0.150	1.00 ± 0.02	14.52 ± 0.75	−1.427 ± 0.107	17.79 ± 2.42	0.537 ± 0.009
	0.155	0.94 ± 0.03	16.30 ± 0.37	−1.462 ± 0.102	26.04 ± 1.16	0.540 ± 0.008
	0.160	0.88 ± 0.01	17.42 ± 0.22	−1.247 ± 0.090	32.08 ± 3.83	0.522 ± 0.008
15	0.146	0.82 ± 0.07	10.09 ± 0.23	−0.666 ± 0.759	10.86 ± 4.93	0.453 ± 0.081
15 (2005)	0.146	0.86 ± 0.08	11.69 ± 0.10	−1.594 ± 0.975	24.54 ± 8.61	0.542 ± 0.073
20 (2005)	0.146	0.56 ± 0.38	10.45 ± 0.33	−0.920 ± 0.982	29.05 ± 11.86	0.479 ± 0.103
30 (2005)	0.146	0.83 ± 0.15	8.01 ± 0.16	−1.383 ± 0.299	69.16 ± 3.88	0.533 ± 0.024
40	0.110	0.47 ± 0.17	3.92 ± 0.50	0.485 ± 0.646	10.51 ± 4.40	0.335 ± 0.112[a]
50	0.093	0.55 ± 0.16	3.42 ± 0.10	−0.159 ± 0.205	31.09 ± 4.70	0.394 ± 0.032

[a] The value calculated only for the cases $\nu < 0$.

3. Results

3.1. Viscosity–time curves at 10 °C

Fig. 1 shows viscosity–time data series for the samples that were gelatinized with different NaOH solution concentrations at 10 °C. In each data series, a large solid diamond indicates the data point with the maximum viscosity. As shown in this figure, an increase in NaOH concentration (0.130–0.160 M) increased the maximum viscosity and shortened the time required to reach it. For example, the viscosity growth at 0.130 and 0.135 M took several hundred minutes to attain the maxima (10–15 mPa·s) but at 0.160 M the maximum of 17–18 mPa·s was reached within 30 min. Note also that the viscosity growth at 0.155 and 0.160 M broke down after arriving at the maxima. This break down phenomenon of viscosity is beyond the limit of the present kinetic analysis. Thus, an equilibrium value (η_G) for each viscosity growth was generally determined by the kinetic analysis applied to the whole data series, but for the cases in which viscosity growth broke down, the kinetic analyses were conducted only for the data series up to their maxima.

The above results suggested that incremental increases in NaOH concentration increased the extent of gelatinization (i.e., starch granule swelling). Above 0.150 M, the swelling power exceeded the limits of maintaining the granular structures of some granules and caused them to be disrupted. These results also suggested that an increase in [NaOH] enhanced the gelatinization rate, which was confirmed by the kinetic analysis.

All the data series up to the maxima conformed to sigmoid curves. Their global shapes were characterized by the positions of IP at which point the curvature of each data series changed in sign and viscosity increased at a maximum rate ($d^2\eta/dt^2 = 0$). To demonstrate the sigmoidal behavior explicitly, it would thus be useful to first show the presence of an IP in a viscosity growth curve. Then, we calculated the rate of viscosity change ($\Delta\eta/\Delta t$) by taking the differences both in time and viscosity between neighboring data points. Due to unavoidable experimental fluctuations, these data series for $\Delta\eta/\Delta t$ plotted against time were more or less scattered, which made it difficult to precisely identify IP. To solve this problem, we used a 5-point smoothing method to make these curves smoother (Lopes da Silva, Gonçalves, & Rao, 1995).

Fig. 2 shows an example of a smoothed data series for the viscosity growth rate for the sample gelatinized with 0.146 M NaOH. This shows a clear maximum point (large open diamond) at t^*[min] = 23.9, which demonstrated the presence of an IP at η^*[mPa·s] = 6.92. Further, if we identify the maximum viscosity

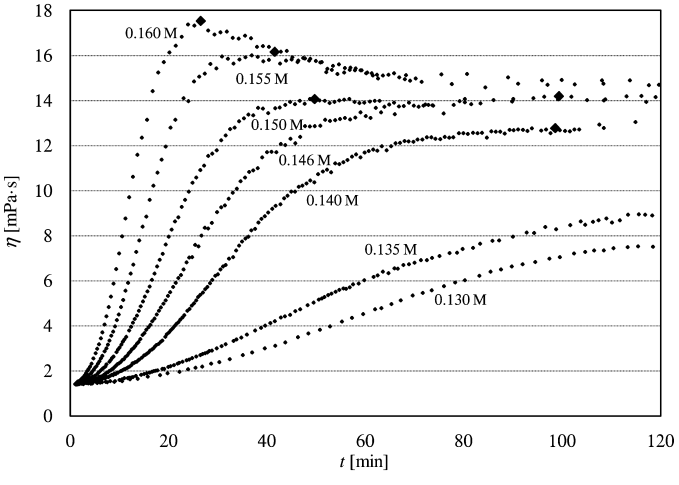

Fig. 1. Viscosity–time data series for 1% rice starch gelatinized with different NaOH solution concentrations at 10 °C. In each data series at 0.140–160 M, the large solid diamond indicates the data point exhibiting the maximum viscosity.

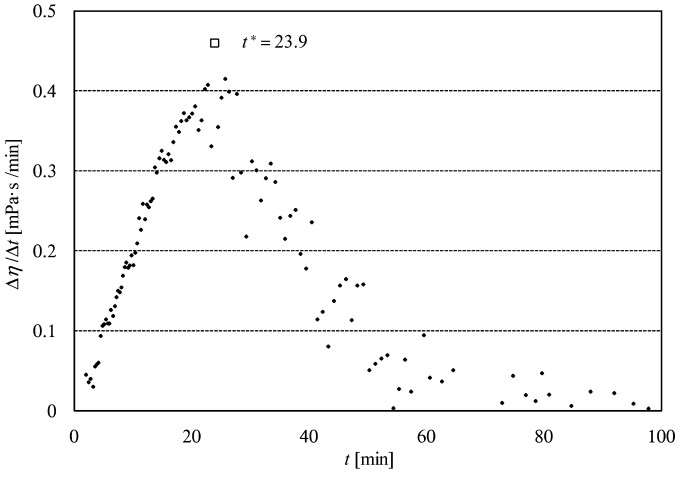

Fig. 2. Data series for the viscosity growth rate ($\Delta\eta/\Delta t$) plotted against time for 1% rice starch gelatinized with a 0.146 M NaOH solution at 10 °C; this was obtained using a 5-point smoothing method. The large open square indicates the maximum point.

(14.2 [mPa·s]) with the equilibrium one η_G[mPa·s], we can estimate the ratio η^*/η_G to be 0.487, from which the mixing exponent was computed through Eq. (3) to be $\nu = -0.874$. However, this estimation of the exponent ν depended only on the viscosities at the maximum point and the IP. It would be better to determine the parameter ν from more detailed information on the viscosity growth data. Thus, we applied a non-linear least-squares method to the whole viscosity growth data series, or to those up to the maximum point in the presence of break down phenomenon. Due to this non-linear regression analysis, 4 parameters η_{UG}, η_G, ν and K in Eq. (2) were estimated simultaneously. Then, the ratio η^*/η_G was calculated from ν through Eq. (3). The results averaged at each NaOH concentration are summarized in Table 1.

Under the change of NaOH concentration, the value of η_G behaved similarly with the maximum viscosity, and η_{UG}[mPa·s] remained almost within 0.09–1.00. The increase of [NaOH] from 0.130 to 0.140 M decreased the mixing exponent ν, thereby increasing the ratio η^*/η_G. As discussed later in this article, we consider these parameters to relate to the degree of complex formation that occurs from the interaction between starch and NaOH. Then, the decrease of ν or the increase of η^*/η_G up to 0.140 M means that the NaOH concentrations of and below 0.135 M were insufficient for the full formation of starch–NaOH complexes. At 0.146 M, these parameters had values of -0.923 ± 0.213 (ν) and 0.491 ± 0.021 (η^*/η_G), which were close to those (-1 for ν and 0.5 for η^*/η_G) having been assumed in previous studies for cold NaOH gelatinization. However, at 0.140 M and 0.150–0.160 M, the mean values of ν were below -1.0 and thereby those of η^*/η_G were above 0.50.

To summarize the results at 10 °C (0.130–0.160 M), the mean of ν ranged from -1.46 to 0.67 and that of the ratio η^*/η_G was distributed over a range of 0.19–0.54. Thus, we confirmed that the value of a mixing exponent ν or that of a ratio η^*/η_G for cold NaOH gelatinization was not limited to the neighborhood of -1.0 (ν) or 0.50 (η^*/η_G) (as assumed in previous studies), but were dispersed over some range even at the same temperature (10 °C).

3.2. Viscosity–time curves at different temperatures

Table 1 also shows the results obtained at 9 °C and 15 °C with a fixed NaOH concentration (0.146 M) and those at 15 °C, 20 °C, and 30 °C for which '(2005)' was added in the first column. The latter results were obtained by reanalyzing our previous data (Yamamoto et al., 2005) using the kinetic method described here. There were some amount of differences in η_G and K between the current and previous samples at 15 °C. Aside from that, both samples exhibited common tendencies for their temperature dependencies. That is, with [NaOH] fixed at 0.146 M, an increase of temperature reduced both η_G values and the time to achieve the maxima of viscosity; the data for the latter are not shown, but the above trend can be discerned from the rate constants in Table 1. However, the ratio η^*/η_G at 0.146 M did not significantly change and remained around 0.50 (0.45–0.54) for different temperatures.

Although the decrease in η_G with increased temperature may contradict general understanding of gelatinization processes in hot water, the following explanation is plausible. From the viscosity data in Table 1 and Fig. 1, we assumed that a fixed NaOH concentration (0.146 M) was sufficient to attain nearly "complete gelatinization" even at 10 °C (i.e., the state at which almost all had starch granules swelled to their limits) without any additional thermal energy. This is in contrast to what occurs in hot water at 60–70 °C for which thermal energy is the sole driving force for gelatinization and is insufficient for complete gelatinization. Thus, a temperature increase from 70 °C to 80 °C results in significant viscosity enhancement (Kubota et al., 1979; Yamamoto et al., 2005). For example, the values of η_G[mPa·s] for 5.0% rice starch were roughly 1 at 60 °C, 4 at 70 °C, 10 at 75 °C, and 60 at 80 °C (Yamamoto et al., 2005).

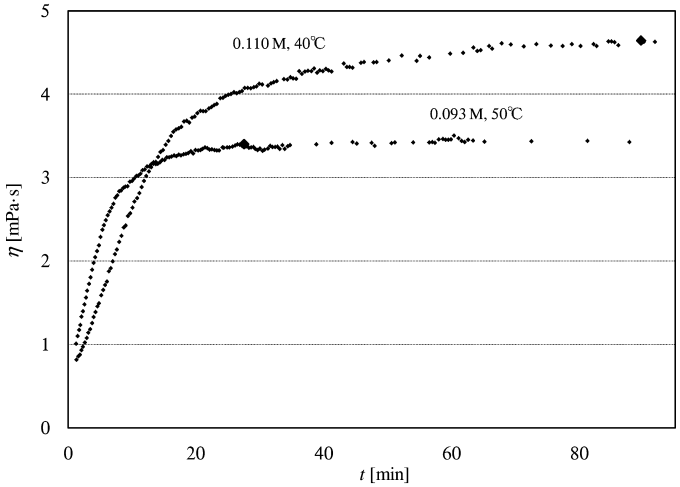

Fig. 3. Viscosity-time data series of 1% rice starch gelatinized with NaOH solutions of 0.110 M at 40 °C and 0.093 M at 50 °C. In each data series, the large solid diamond indicates the data point with the maximum viscosity.

In the current case of NaOH-induced gelatinization, the viscosity of a starch dispersion may be more largely affected by the dispersing medium (NaOH–water system) than by the swelling state of dispersoid particles (rice starch granules), which are assumed to be nearly saturated at 0.146 M. An increase in temperature decreases the mean cluster size of water molecules and electrolytes and reduces the viscosity of the dispersing medium. For the current case, this effect may exceed the promoting effect of granule swelling.

Another explanation could be that granule swelling itself is suppressed at higher temperatures. The swelled starch particles in NaOH gelatinization should have an internal structure that is different from those in purely hot-water gelatinization, and the swelling mechanism itself could be different. In any case, this is an issue to be pursued by future studies.

At temperatures higher than 30 °C, viscosity increased very rapidly to identify an IP; thus, the samples were gelatinized with NaOH solutions of 0.110 M at 40 °C and 0.093 M at 50 °C. The resulting viscosity–time data series (Fig. 3) conformed to sigmoid curves, but with much smaller values of η_G and η^* than those at lower temperatures and with higher NaOH concentrations, although η^*/η_G ratios were not so small (Table 1). These samples that were gelatinized at 40 °C and 50 °C were influenced by more thermal energy than those at lower temperatures; however the NaOH concentrations were quite insufficient for complete gelatinization. As inferred from the reaction rates in Table 1, thermal energy accelerated the progress of gelatinization, although the extent of gelatinization was small (i.e., the reaction might remain in the amorphous region and not achieve the crystallite melting).

3.3. Uniform rate constants

As described above, all viscosity–time data series obtained in this study conformed to sigmoid curves with IPs. Their global shapes were classified by the IP positions relative to the equilibrium points, which were calculated theoretically from the mixing exponent (ν) in the kinetic model.

The kinetic analysis was conducted using non-linear least-squares method to provide a value of reaction rate constant K, in addition to those of η_{UG}, η_G and ν. These parameters were defined uniformly over the entire region of each data series or those up to

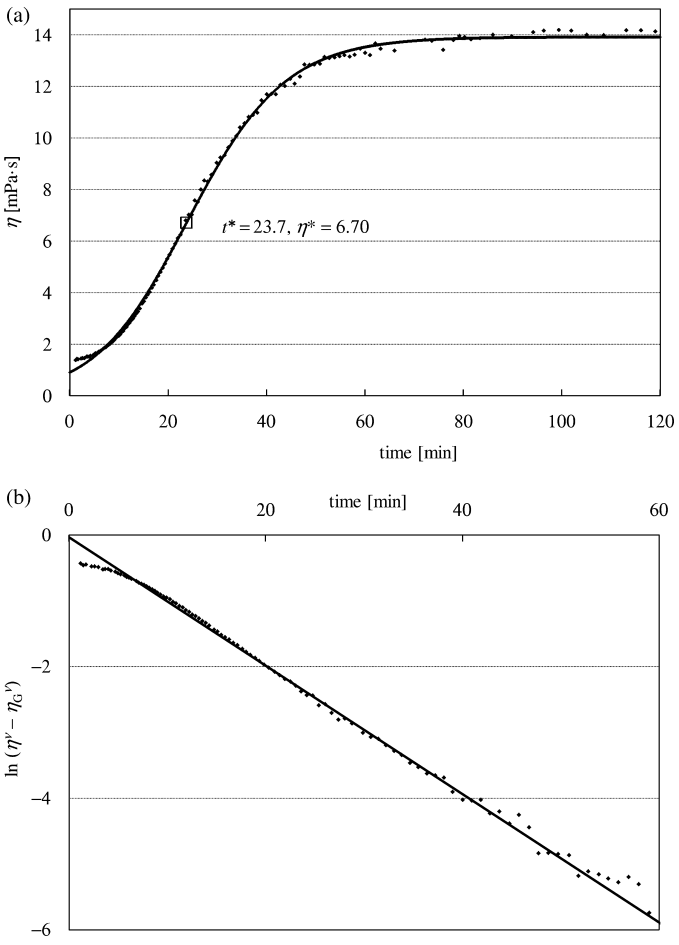

Fig. 4. (a) Viscosity–time data series of 1% rice starch gelatinized with a 0.146 M NaOH solution at 10 °C along with the theoretical curve (solid curve) determined by a uniform kinetic analysis, and (b) the linearized data series along with the theoretical line (solid line). In (a), the curve fitting was done by means of a non-linear least-squares method, and a large open square indicates the IP position estimated from the kinetic analysis.

the maximum viscosity, and thus obtained value of K represented a mean reaction rate for each overall gelatinization process.

Fig. 4(a) illustrates an example of applying uniform kinetic analysis to the data series obtained with a 0.146 M NaOH solution at 10 °C. This analysis gave $\eta_{UG} = 0.91$, $\eta_G = 13.9$, $\nu = -0.814$ and $K[\times 10^{-2}\ \mathrm{min}^{-1}] = 9.76$, and led to $\eta^*/\eta_G = 0.481$. These results for ν and η^*/η_G were close to those ($\nu = -0.874$ and $\eta^*/\eta_G = 0.487$) estimated by the IP analysis in Section 3.1.

Aside from the initial region ($1.2 < t < 4.2$), a theoretical curve generated from the kinetic model (2) with 4 parameters substituted by the above values provided a globally good fit to the measured data series (Fig. 4(a)), which supported the overall validity of this analysis. This uniform analysis was repeated for all data series, including those previously generated, and provided a well fit to each data series. The uniform rate constant K could thus be used as a single parametric value that was representative of each data series for comparisons among the reaction rates for different gelatinization conditions. The results are listed in the K column of Table 1.

From this column, the following two trends were noticed. The first trend was the dependence on NaOH concentration. An increase in [NaOH] generally enhanced the rate constant. Under an isothermal condition (10 °C), this [NaOH] dependence was approximated by the power-law rule:

$$K \propto [\mathrm{NaOH}]^{17.2} \quad (R^2 = 0.919). \tag{6}$$

A second trend was the dependence on temperature. Although we did not systematically examine this, the results in Table 1 showed a tendency that a temperature increase accelerated the reaction. Even with lower NaOH concentrations (0.110 and 0.093 M), K had larger values due to the higher temperatures (40 °C and 50 °C) than that with 0.135 M at 10 °C.

3.4. Kinetic analysis with a non-uniform rate constant

As exemplified in Fig. 4(a), our kinetic model provided a well description for the overall behaviors of all the viscosity growth data series (up to the maximum point) obtained in this study. However, a careful comparison between experimental and theoretical data showed slight differences between them. For example in Fig. 4(a), a difference was found in the very early stage ($t \le 4$) of gelatinization, and a theoretical curve yielded an erroneously smaller η_{UG}.

From our hypothesis developed in Section 4, we believe that this difference originated in the complex formation that occured in starch granules. That is, at the beginning of NaOH gelatinization, some NaOH was consumed in the complex formation. Due to such effect, the concentration of free NaOH inside starch granules, which is effective for destructing hydrogen bonds (i.e., the progression of gelatinization), was reduced during some early stages. This reduction of effective [NaOH] could result in lowering of reaction rate.

The reduction of a rate constant in the very early stage can be more clearly suggested in Fig. 4(b), in which both experimental and theoretical data in Fig. 4(a) were linearized by using Eq. (4). For this sample, the local slope of the linearized data during the period $t \le 4$ is smaller than that of the line derived by the uniform analysis, while that during the period around $t = 20$ appears to be a little bit larger. The actual gelatinization rate might vary more or less with time. Even for a pure starch–water system, it has been suggested that gelatinization process consists of several stages (Katsuta, 1996). If NaOH gelatinization is also a multistage process (as naturally expected from the above hypothesis), there is no reason to insist that a whole process must be controlled by a uniform rate constant.

If there is a change with time in the reaction rate, it must reflect the details of the gelatinization process and the underlying mechanism. Therefore, it would be desirable if we could obtain such information by refining the kinetic method. In this subsection, we will develop our kinetic method further to incorporate a change in the rate constant and apply this to the current data. Since we do not have sufficient space remaining in this article, a detailed derivation of the kinetic equations and the results will be presented in a future article. Here we only provide an outline of this new approach and an example of the results. The main idea is to disassemble the entire gelatinization process into several elementary stages, each of which could have a rate constant value that is independent of the others.

Suppose that the entire process consists of $n(\ge 2)$ elementary stages, where the i-th stage ($i = 1, 2, \ldots, n$) over a time interval $t_i \le t \le t_i'$ is characterized by a degree x_i of gelatinization, viscosity η_i, and a rate constant K_i. Between the $(i-1)$-th and the i-th stages ($2 \le i \le n$), a continuity condition of $x_{i-1} = x_i$ is imposed at the intermediate time of $t_{i-1,i} \equiv (t_{i-1}' + t_i)/2$ of these neighboring stages in order to solve the rate equation for the degree (x_i) of gelatinization. The viscosity in the first stage is given by Eq. (2): $\eta_1^\nu(t) = \eta_G^\nu + \eta_{UGG}^\nu\, e^{-K_1 t}$. Then, using the continuity condition, the time evolution of η_i for the $i(\ge 2)$-th stage is derived iteratively by

$$\eta_i^\nu(t) = \eta_G^\nu + \eta_{UGG}^\nu \exp\left(-K_1\, t_{1,2} - \sum_{j=2}^{i-1} K_j \left(t_{j,j+1} - t_{j-1,j}\right) - K_i \left(t - t_{i-1,i}\right)\right). \tag{7}$$

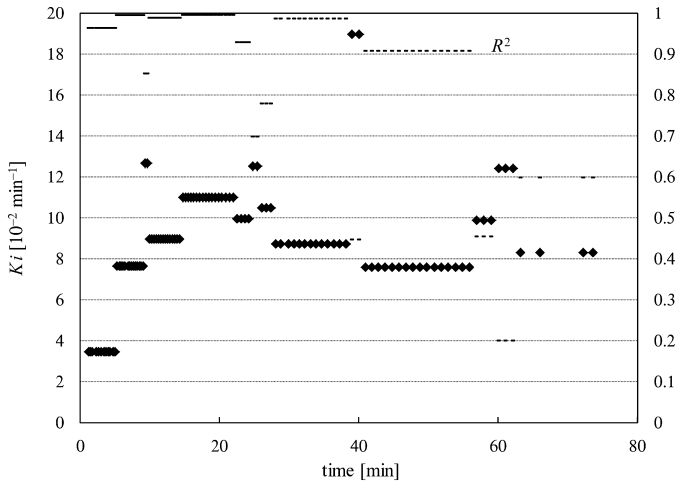

Fig. 5. Time distributions of non-uniform rate constants K_i (solid diamonds) and R^2 values (bars) for the sample gelatinized with a 0.146 M NaOH solution at 10 °C. This result was obtained by the non-uniform kinetic analysis using a linear regression method.

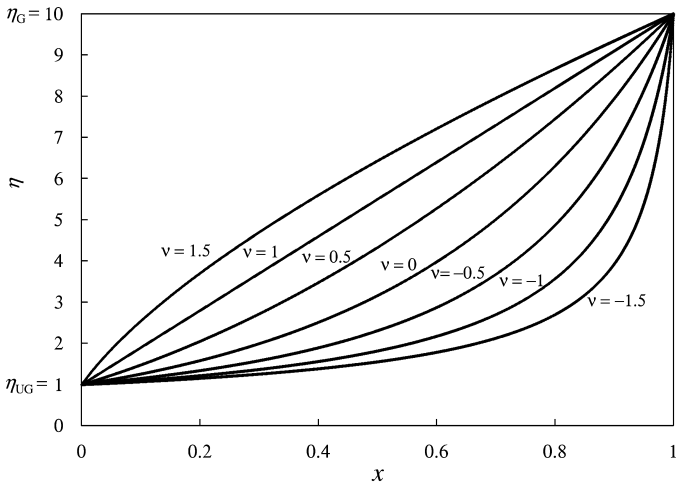

Fig. 6. Relationships between viscosity η and the degree of gelatinization x determined from the power-law mixing rule with: $\nu = -1.5, -1, -0.5, 0, 0.5, 1.0$, and 1.5, where η_{UG} and η_G were set at 1 and 10, respectively.

For the actual kinetic analysis, the entire data series was divided into several stages such that each process ($t_i \le t \le t_i'$) could be fitted to Eq. (7) with a movable end point t_i'. The parameters ν and η_G were previously fixed at the values obtained from the advanced uniform analysis. Then from the fitting to the first stage, the parameters η_{UG}, K_1 and t_1' (t_2) were determined. The subsequent fitting procedure to the remaining data provided K_i and t_i' (t_{i+1}) iteratively ($2 \le i$).

Fig. 5 shows the result for the change in the rate constant obtained by applying the above non-uniform analysis to the data series shown in Fig. 4. In the data fitting procedure, the linear regression analysis was used for the linearized data series (Fig. 4(b)) so that each fitting and disassembling of the data series provided the highest degree of linearity (i.e., the maximum R^2) in each stage. The slope of each regression line provided the rate constant K_i for each stage. Note that from the functional property of the logarithm the linearized data ($\ln(\eta^\nu - \eta_G^\nu)$) tended to be scattered inevitably and the reliability of the analysis was lost near the equilibrium ($\eta \approx \eta_G$). However, this method could provide the results much more efficiently than non-linear regression analysis and could be reliable at least in the region far from the equilibrium.

The result in Fig. 5 revealed >10 elementary stages with different rate constants, depending on the stage. During the first stage (t[min] < 5.1), gelatinization proceeded with K_1 [$\times 10^{-2}$ min^{-1}] = 3.46, which was much smaller than the uniform value (K = 9.76), as expected from Fig. 4. The gelatinization then accelerated and progressed during the second stage ($5.1 < t < 9.2$) with $K_2 = 7.63$, which was still $< K$. Then, roughly speaking, a rate constant increased step by step and reached the stage ($14.5 < t < 22.2$) with the maximum value ($11.0 > K$). Subsequently, a rate constant tended to reduce slowly to the minimum value ($7.60 < K$) recorded at the stage during the period $40.5 < t < 50.4$.

4. Discussion

The sigmoid curves for the viscosity growth measured for NaOH starch gelatinization can be comprehensively described in terms of a first-order kinetic model with a general power-law mixing rule (1). In this scheme, the exponent ν(< 1) determines the global shape of a growth curve, i.e., the ratio of the viscosity at IP (η^*) to the equilibrium value (η_G).

From the perspective of this general scheme, the models used in previous studies corresponded to two special cases: the case with $\nu = 1$ ($\eta^*/\eta_G = 0$) applied to gelatinization in hot water and the case with $\nu = -1$ ($\eta^*/\eta_G = 0.50$) applied to gelatinization in cold NaOH solutions at specified concentrations. For the latter processes, using the model with $\nu = -1$ was not poor. However, our general scheme allowed us to select a model (ν) that had a better fit to experimental data obtained for gelatinization under general conditions. Further refining this analysis method by decomposing the process provided information on the evolution of the reaction rate.

The current experiment demonstrated the existence of gelatinization phenomena that were characterized by widely ranging values of ν or η^*/η_G (Table 1). From the functional property of Eq. (3), an increase in η^*/η_G reduced the exponent ν. For example, we observed that at an isothermal condition (10 °C), an increase in [NaOH] from 0.130 to 0.140 M increased the η^*/η_G ratio, thereby reducing the mixing exponent (ν). The physical meaning of this result can be understood from the mixing rule of viscosity (1).

Fig. 6 shows the relationship between viscosity, η, and the degree of gelatinization, x, determined from the power-law mixing rule with $\nu = -1.5, -1, -0.5, 0, 0.5, 1.0$, and 1.5 for the case when η_{UG} and η_G are set to 1 and 10, respectively. With an increase of x from 0 to 1 (progression of gelatinization), the viscosity η increases from the common initial value ($\eta_{UG} = 1$) to the common equilibrium value ($\eta_G = 10$) through different paths depending on ν. Viscosity increases linearly for the case $\nu = 1$ and in a concave manner for the case $\nu < 1$ (the case when the viscosity–time curve is able to have an IP). Thus, different values of ν result in different values of viscosity taken at any midpoint ($0 < x < 1$) of the gelatinization process.

During this process, a sample's viscosity is determined by blending low viscosity η_{UG} and high viscosity η_G through the mixing rule (1) with an exponent ν. As seen in Fig. 6, a decrease in ν reduces the total viscosity at any fixed degree ($0 < x < 1$) of gelatinization. This means that at lower ν (higher η^*/η_G), the gelatinized part (G) with a high viscosity (η_G) would have less of an effect on the viscosity (η) of the whole sample (UG+G). In other words, a higher η^*/η_G ratio implies a higher rheological independency for G.

In this way, a mixing exponent, ν, or the η^*/η_G ratio is an index parameter that indicates the magnitude of the influence of G on the viscosity of the total system (UG + G). Recall that the choice of $\nu = 1$ was realized for gelatinization in hot water for which a semi-cooperative property was expected, as argued by Marchant and Blanshard and by French.

Therefore, we infer that the rheological independency ($\nu < 1$) observed for NaOH gelatinization was induced by structural independence and that promising candidates of these structurally

independent objects are starch *complexes* (Tomasik & Schilling, 1998) that are formed inside starch granules during gelatinization. These complexes would reduce the semi-cooperativity of gelatinization, which would decrease the mixing exponent ν and increase the η^*/η_G ratio of viscosity–time curves.

For the present case of NaOH gelatinization, we previously proposed two types of complex formation (Yamamoto et al., 2006; Yamamoto, Kawakami, et al., 2012). One is a starch–sodium complex formed through a cation exchange: St.-OH + NaOH → St.-ONa + H_2O, which could arise at the hydroxyl groups of starch chains (Oosten, 1982, 1983, 1990) and should occur irrespective of the differences between amylose and amylopectin. This type of complex formation has long been known as a type of metal adsorption phenomena of starch (Leach, Schoch, & Chessman, 1961; Rakowski, 1913).

Another type of complex formation could arise primarily for starches containing amylose with lipids. Amylose is known to form inclusion complexes with numerous types of compounds including lipids, inside a helical structure. Native starches of the non-glutinous type usually contain lipids included in amylose, some of which are free fatty acids like palmitic and linoleic acids in rice starches. Then, even at low temperatures, NaOH penetrating into the starch granules could react with these free higher fatty acids to generate sodium salts of higher fatty acids. This reaction is a simple neutralization and can occur without prolonged heating, as is usually required for the saponification of triglycerides. These sodium salts of higher fatty acids have both large hydrophobic groups and hydrophilic groups and could act as strong surfactants. They could then form strong complexes primarily with amylose, which are stable at low temperatures.

These two types of complexes formed in the gelatinized part of starches would enhance its structural independence, which would result in reducing the semi-cooperative nature.

5. Conclusions

Continuous capillary viscometry was used to analyze 1% rice starches gelatinized with different NaOH solution concentrations at different temperatures. The measured viscosity–time data series generally conformed to sigmoid curves that had IPs at arbitrary positions. Using a first-order kinetic model with a power-law mixing rule provided a comprehensive classification of these curves for which the mixing exponent ν could be used as a classification parameter and had a one-to-one correspondence with the ratio of viscosity at IP (η^*) to the equilibrium value (η_G). The observed viscosity growth processes were characterized by widely distributed values for these parameters. The mean ν value ranged from −1.59 to 0.67 and that for η^*/η_G ranged from 0.19 to 0.54.

The uniform kinetic analysis showed that the reaction rate at 10 °C increased with an increase in the NaOH concentration and was power-law dependent. Furthermore, the results suggested that gelatinization progressed non-uniformly over time. We then used a non-uniform analysis by decomposing the entire gelatinization process into several elementary stages with different rate constant values. This revealed, for example at 0.146 M (10 °C), that gelatinization started with a small rate and was accelerated during the early stages to attain a maximum rate at an intermediate stage.

Thus, our kinetic scheme allowed us to perform both a unified treatment over a wide range of measured data series and a minute analysis of each data series. An interpretation of our kinetic model showed that the derived classification parameter (mixing exponent ν or the η^*/η_G ratio) could be used as an index parameter for the magnitude of the rheological independency of the gelatinized part. From this perspective, we inferred that the sigmoid property of the viscosity growth curves was caused by two types of complexes that formed inside starch granules during the early stage of gelatinization.

References

French, D. (1984). Organization of starch granules. In R. L. Whistler, E. F. Paschall, & J. N. Bemiller (Eds.), *Starch: Chemistry and Technology* (2nd ed., pp. 183–247). New York: Academic Press.

Hebeish, A., EI-Thalouth, I. A., & EI-Kashouti, M. (1981). Gelatinization of rice starch in aqueous urea solutions. *Starch/Stärke*, *33*, 84–90.

Jane, J.-L. (1993). Mechanism of starch gelatinization in neutral salt solutions. *Starch/Stärke*, *45*, 161–166.

Katsuta, K. (1996). Dynamic viscoelastic behavior of rice starch suspension on the gelatinization process. *Journal of Applied Glycoscience*, *43*, 541–543.

Kubota, K., Hosokawa, Y., Suzuki, K., & Hosaka, H. (1979). Studies on the gelatinization rate of rice and potato starches. *Journal of Food Science*, *44*, 1394–1397.

Leach, V. H. W., Schoch, T. J., & Chessman, E. F. (1961). Adsorption von alkalien durch das Stärkekorn. *Die Stärke*, *13*, 200–203.

Lopes da Silva, J. A., Gonçalves, M. P., & Rao, M. A. (1995). Kinetics and thermal behaviour of the structure formation process in HMP/sucrose gelation. *International Journal of Biological Macromolecules*, *17*, 25–32.

Lund, D. (1984). Influence of time, moisture, ingredients, and processing conditions on starch gelatinization. *CRC Critical Reviews in Food Science and Nutrition*, *20*, 249–273.

Marchant, J. L., & Blanshard, J. M. V. (1978). Studies of the dynamics of the gelatinization of starch granules employing a small angle light scattering system. *Starch/Stärke*, *30*, 257–264.

Oosten, B. J. (1982). Tentative hypothesis to explain how electrolytes affect the gelatinization temperature of starches in water. *Starch/Stärke*, *34*, 233–239.

Oosten, B. J. (1983). Explanations for phenomena arising from starch–electrolytes interactions. *Starch/Stärke*, *35*, 166–169.

Oosten, B. J. (1990). Interactions between starch and electrolytes. *Starch/Stärke*, *42*, 327–330.

Rakowski, V. A. (1913). Zur kenntnis der adsorption. VII. Adsorption und hydrolyse. *Kolloid-Z*, *12*, 177–181.

Shon, K.-J., Lim, S.-T., & Yoo, B. (2005). Rheological properties of rice starch dispersions in dimethyl sulfoxide. *Starch/Stärke*, *57*, 363–369.

Tomasik, P., & Schilling, C. H. (1998). Complexes of starch with inorganic guests. *Advances in Carbohydrate Chemistry and Biochemistry*, *53*, 263–343.

Vermeylen, R., Derycke, V., Delcour, J. A., Goderis, B., Reynaers, H., & Koch, M. H. J. (2006). Gelatinization of starch in excess water: beyond the melting of lamellar crystallites. A combined wide- and small-angle X-ray scattering study. *Biomacromolecules*, *7*, 2624–2630.

Woodside, W., & Messmer, J. H. (1961). Thermal conductivity of porous media, I. Unconsolidated sands. *Journal of Applied Physics*, *32*, 1688–1699.

Yamamoto, H. (2006). Kinetics of observable with power-law mixing rule in the first-order reaction process. *Japan Journal of Food Engineering*, *7*, 245–248.

Yamamoto, H., Isozumi, N., & Sugitani, T. (2005). A concavity property of the viscosity growth curve during alkali gelatinization of rice starch. *Carbohydrate Polymers*, *62*, 379–386.

Yamamoto, H., Kawakami, A., Kitagawa, A., & Yamagata, S. (2012). Batch-type cone-plate viscometry of corn and wheat starches gelatinized by NaOH solution at 20 °C. *Journal of Applied Glycoscience*, *59*, 125–130.

Yamamoto, H., Makita, E., Oki, Y., & Otani, M. (2006). Flow characteristics and gelatinization kinetics of rice starch under strong alkali conditions. *Food Hydrocolloids*, *20*, 9–20.

Yamamoto, H., Moriyasu, M., Nagase, M., Nakagawa, Y., Nakamura, Y., & Oka, M. (2012). Capillary viscometry of corn and wheat starches gelatinized by NaOH solutions at room temperatures. *Current Trends in Polymer Science*, *16*, 15–22.